

¹ Introduction

² Siphonophores have fascinated zoologists for centuries for their extremely subspecialized
³ colonial organization and integration. Today we have a comprehensive taxonomic coverage
⁴ on the morphological diversity of this group due to the extensive work of siphonophore
⁵ taxonomists in the past few decades (Pugh 1983, 2001; Pugh and Harbison 1986; Pugh
⁶ and Youngbluth 1988; Dunn et al. 2005; Haddock et al. 2005; Hissmann 2005; Bardi and
⁷ Marques 2007; Pugh and Haddock 2010; Pugh and Baxter 2014), which has been elegantly
⁸ synthesized in detailed synopses (Totton and Bargmann 1965; Mapstone 2014). In addition,
⁹ recent advances in phylogenetic analyses of siphonophores (Munro et al. 2018; Damian-
¹⁰ Serrano et al. 2020) have provided a macroevolutionary context to interpret this diversity.
¹¹ With these assets in hand, we can now begin to study siphonophores from an orthogonal
¹² perspective, focusing on the diversity and evolutionary history of specific structures. Here we
¹³ focus on one of such structures: the tentilla. Like many cnidarians, siphonophore tentacles
¹⁴ bear side branches (tentilla) with nematocysts (Fig. 1C-E). But unlike other cnidarians,
¹⁵ most siphonophore tentilla are dynamic structures that react to prey encounters by rapidly
¹⁶ unfolding the nematocyst battery to slap around the prey (Fig. 1F). This maximizes the
¹⁷ surface area of contact between the nematocysts and the prey they fire upon. In addition,
¹⁸ siphonophore tentilla present a remarkable diversity of morphologies (Fig. 2), sizes, and
¹⁹ nematocyst complements (Fig. 3). Our overarching aim is to organize all this phenotypic
²⁰ diversity in a phylogenetic context, and identify the evolutionary processes that generated it.

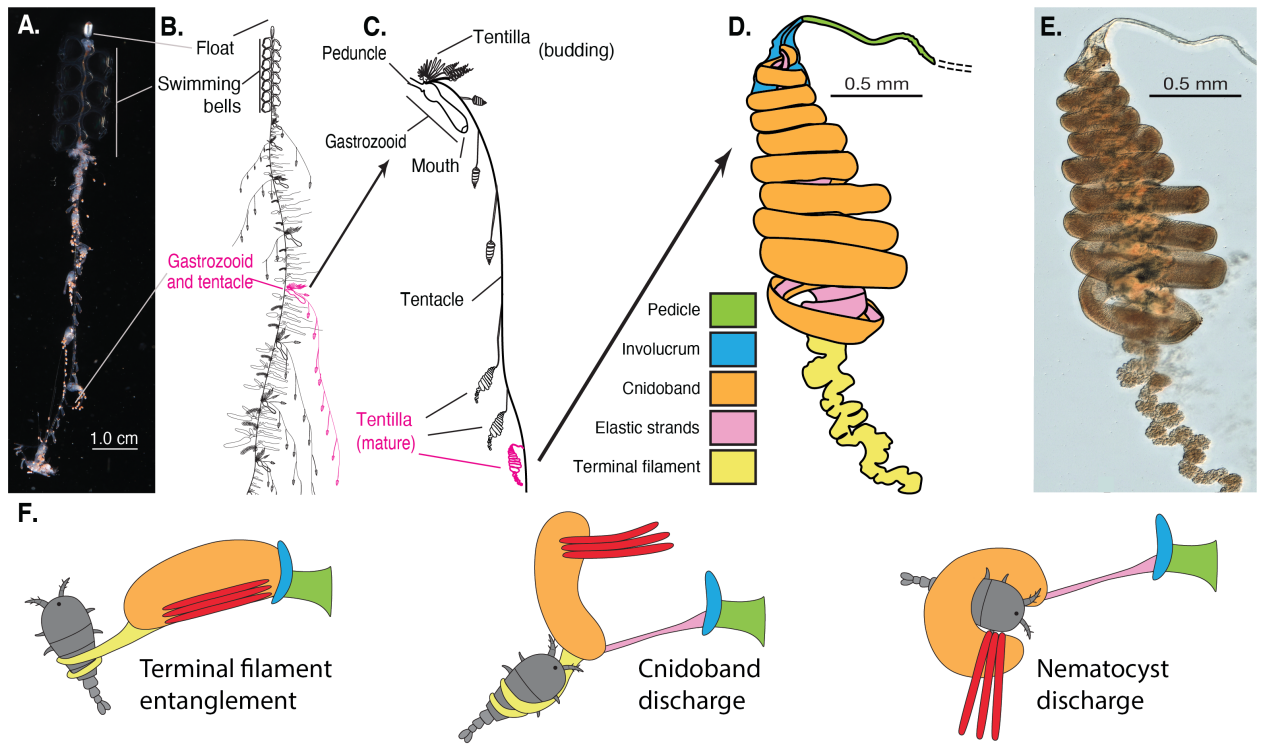


Figure 1: Siphonophore anatomy. A - *Nanomia* sp. siphonophore colony (photo by Catriona Munro). B, C - Illustration of a *Nanomia* colony, gastrozoid, and tentacle closeup (by Freya Goetz). D - *Nanomia* sp. Tentillum illustration and main parts. E - Differential interference contrast micrograph of the tentillum illustrated in D. Figure reproduced from Damian-Serrano et al. 2020 with permission. F. Action strip showing the behavior of tentilla during prey capture, illustrated by Riley Thompson.

21 In Damian-Serrano et al. (2020), we collected the most extensive morphological dataset
22 on siphonophore tentilla and nematocysts using state-of-the-art microscopy techniques, and
23 expanded the taxon sampling of the phylogeny to disentangle the evolutionary history. The
24 analyses we carried out led to novel, generalizable insights into the evolution of pred-
25 atory specialization. The primary findings of that work were that generalists evolved from
26 crustacean-specialist ancestors, and that feeding specializations were associated with distinct
27 modes of evolution and character integration patterns. The work we present here is comple-
28 mentary to Damian-Serrano et al. (2020), showcasing a far more detailed account on the
29 evolutionary history of tentilla morphology.

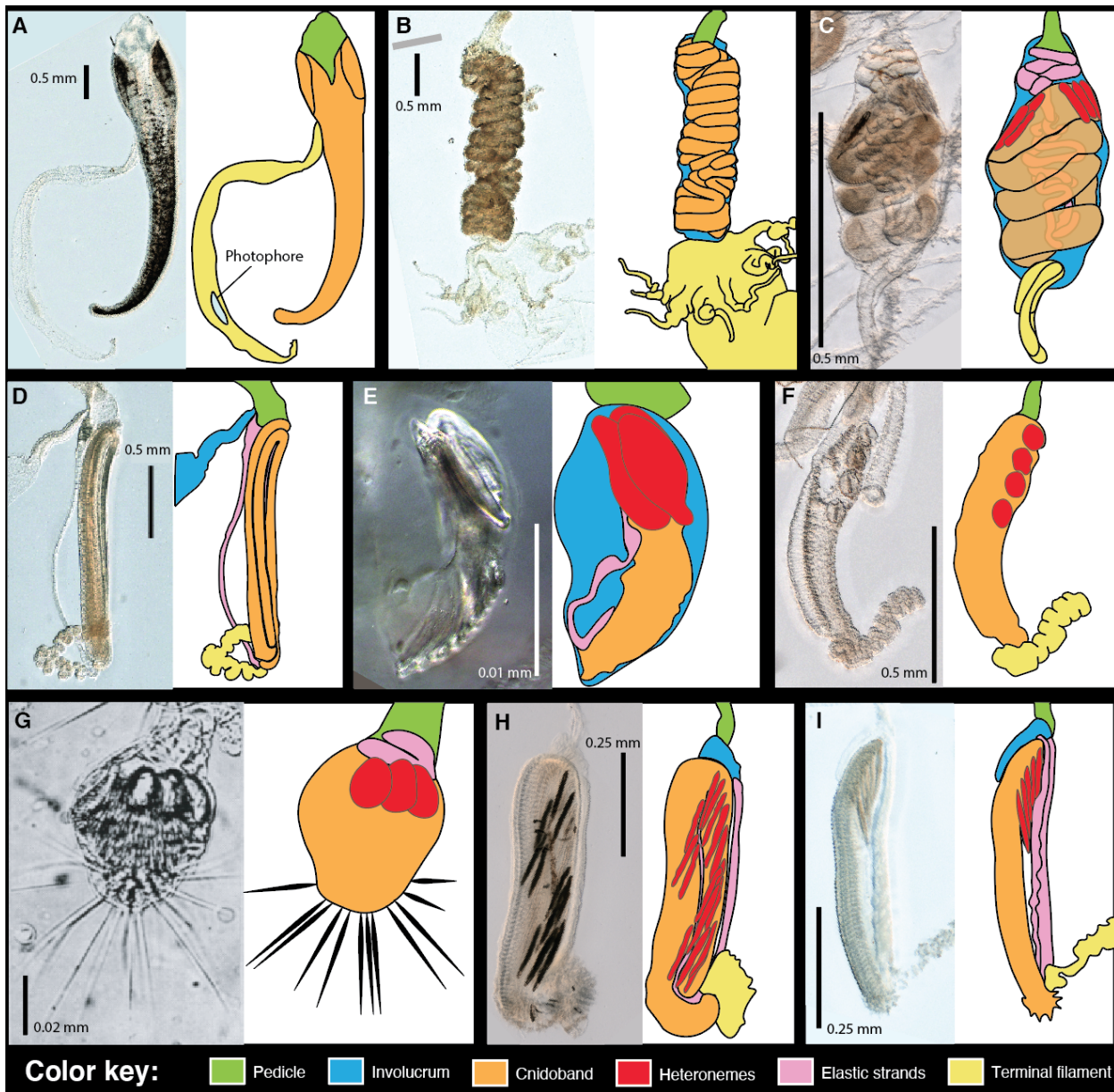


Figure 2: Tentillum diversity. The illustrations delineate the pedicle, involucrum, cnidoband, elastic strands, terminal structures. Heteroneme nematocysts (stenoteles in C,E,F,G and mastigophores in H,I) are only depicted for some species. A - *Erenna laciiniata*, 10x. B - *Lychnagalma utricularia*, 10x. C - *Agalma elegans*, 10x. D - *Resomia ornicephala*, 10x. E - *Frillagalma vityazi*, 20x. F - *Bargmannia amoena*, 10x. G - *Cordagalma* sp., reproduced from Carré 1968. H - *Lilyopsis fluoracantha*, 20x. I - *Abylopsis tetragona*, 20x.

30 Nematocysts are unique biological weapons for defense and prey capture exclusive to
31 the phylum Cnidaria. Mariscal (1974) reported that hydrozoans have the largest diversity
32 of nematocyst types among cnidarians. Among them, siphonophores present the greatest
33 variety of types (Mapstone 2014), and vary widely across taxa in which and how many types
34 they carry on their tentacles (Fig. 3). Werner (1965) noted that there are nine types of
35 nematocyst found in siphonophores, of which four, anacrophore rhopalonemes, acrophore
36 rhopalonemes, homotrichous anisorrhizas, and birhopaloids, are unique to them. Heteroneme
37 and haploneme nematocysts serve penetrant and entangling functions, while rhopalonemes
38 and desmonemes work by adhering to the surface of the prey. While recent descriptive
39 studies have expanded and confirmed our understanding of this diversity, the evolutionary
40 history of nematocyst type gain and loss in siphonophores remains unexplored. Thus, here
41 we reconstruct the evolution of shifts, gains, and losses of nematocyst types, subtypes, and
42 other major categorical traits that led to the extant diversity we see in siphonophore tentilla.

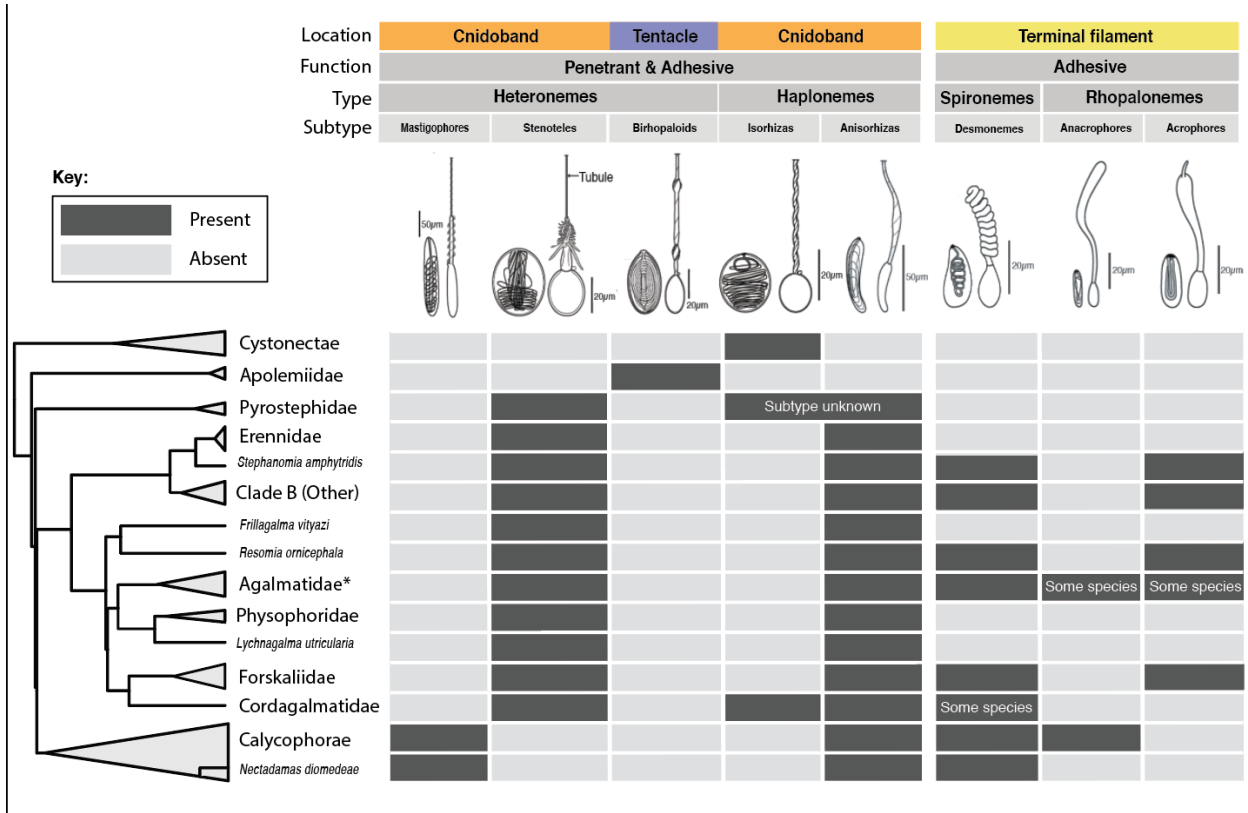


Figure 3: Phylogenetic distribution of nematocyst types, subtypes, functions, and locations in the zooid across the major siphonophore clades. Illustrations reproduced with permission from Mapstone (2014). Undischarged capsules to the left, discharged to the right. Agalmatidae* here refers only to the genera *Agalma*, *Athorybia*, *Halistemma*, and *Nanomia*.

43 Distantly related organisms that evolved to feed on similar resources often evolve similar
44 adaptations (Winemiller et al. 2015). In Damian-Serrano et al. (2020), we found strong
45 associations between piscivory and haploneme shape across distantly related siphonophore
46 lineages. These associations could have been produced by convergent changes in the adaptive
47 optima of these characters. Here we set out to test this hypothesis using comparative
48 model fitting methods. Analyzing the diversity of morphological states from a phylogenetic
49 perspective allows us to identify the specific evolutionary processes that gave rise to it. Here
50 we fit and compare a variety of macroevolutionary models to siphonophore tentilla morphology
51 measurement data to identify instances of neutral divergence, stabilizing selection, changes in
52 the speed of evolution, and convergent evolution.

53 In Damian-Serrano et al. (2020) we fit discriminant analyses to identify characters that are
54 predictive of feeding guild. These discriminant analyses can be used to generate hypotheses
55 on the diets of ecologically understudied siphonophore species for which we have morphology
56 data. Here we present a Bayesian prediction for the feeding guild of 45 species using the
57 discriminant functions and morphological dataset in Damian-Serrano et al. (2020). As
58 mentioned above, tentilla are far from being ornamental shapes and are in fact violently
59 reactive weapons for prey capture (Mackie et al. 1987; Damian-Serrano et al. 2020). While
60 we now have detailed characterizations of tentilla morphologies across many species, the
61 diversity of dynamic performances and their relationships to the undischarged morphologies
62 have not been examined to date. To address this gap, we set out to record high-speed video
63 of the *in vivo* discharge dynamics of several siphonophore species at sea, and compare the
64 kinematic attributes to their morphological characters.

65 Methods

66 All character data and the phylogeny analyzed here were published in Damian-Serrano et al.
67 (2020). Details on the specimen collection, microscopy, and measurements can be found in the
68 aforementioned publication. To facilitate access, we re-included here the character definitions

69 (SM15) and specimen list (SM16) in the Supporting Information. We log-transformed all
70 the continuous characters that did not pass Shapiro-Wilks normality tests, and used the
71 ultrametric constrained Bayesian time tree in all comparative analyses. Inapplicable characters
72 were recorded as NA states, and species with states that could not be measured due to
73 technical limitations were removed before the analyses. We used the feeding guild categories
74 detailed in Damian-Serrano et al. (2020) with one modification: including all *Forskalia* spp.
75 as generalists instead of as a single *Forskalia* species on the tree after a reinterpretation of the
76 data in Purcell (1981). In order to characterize the evolutionary history of tentilla morphology,
77 we fitted different models generating the observed data distribution given the phylogeny for
78 each continuous character using the function fitContinuous in the R package *geiger* (Harmon
79 et al. 2007). These models include a non-phylogenetic white-noise model (WN), a neutral
80 divergence Brownian Motion model (BM), an early-burst decreasing rate model (EB), and
81 an Ornstein-Uhlenbeck (OU) model with stabilizing selection around a fitted optimum trait
82 value. In the same way as Damian-Serrano et al. (2020), we then ordered the models by
83 increasing parametric complexity, and compared their corrected Akaike Information Criterion
84 (AICc) scores (Sugiura 1978). We used the lowest (best) score with a delta of 2 to determine
85 significance relative to the next simplest model (SM10). We calculated model adequacy scores
86 using the R package *arbutus* (Pennell et al. 2015) (SM11), and calculated phylogenetic signals
87 in each of the measured characters using Blomberg's K (Blomberg et al. 2003) (SM10). To
88 reconstruct the ancestral character states of nematocyst types and other categorical traits
89 (character matrix available in Supplementary Information), we used stochastic character
90 mapping (SIMMAP) using the package *phytools* (Revell 2012).

91 In order to examine the degree of phenotypic integration within the tentillum, we explored
92 the correlational structure among continuous characters and among their evolutionary histories
93 using principal component analysis (PCA) and phylogenetic PCA (Revell 2012). Since the
94 character dataset contains gaps due to missing data and inapplicable character states (SM14),
95 we carried out these analyses on a subset of species and characters that allowed for the most

96 complete dataset. This was done by removing the terminal filament characters (which are
97 only shared by a small subset of species), and then removing species which had inapplicable
98 states for the remaining characters (apolemiids and cystonects). In addition, we obtained
99 the correlations between the phylogenetic independent contrasts (Felsenstein 1985) using
100 the package *rphylip* (Revell and Chamberlain 2014) accounting for intraspecific variation.
101 Using these contrasts, we identified multivariate correlational modules among characters. To
102 test and quantify phenotypic integration between these multivariate modules, we used the
103 phylogenetic phenotypic integration test in the package *geomorph* (Adams et al. 2016).

104 When comparing the morphospaces of species in different feeding guilds, we carried out
105 a PCA on the complete character dataset while transforming inapplicable states of absent
106 characters to zeros (i.e. cnidoband length = 0 when no cnidoband is present) to account
107 for similarity based on character presence/absence. Using these principal components, we
108 examined the occupation of the morphospace across species in different feeding guilds using a
109 phylogenetic MANOVA with the package *geiger* (Harmon et al. 2007) to assess the variation
110 explained, and a morphological disparity test with the package *geomorph* (Adams et al. 2016)
111 to assess differences in the extent occupied by each guild.

112 In order to detect and evaluate instances of convergent evolution, we used the package
113 SURFACE (Ingram and Mahler 2013). This tool identifies OU regimes and their optima
114 given a tree and character data, and then evaluates where the same regime has appeared
115 independently in different lineages. We applied these analyses to the haploneme nematocyst
116 length and width characters as well as to the most complete dataset without inapplicable
117 character states.

118 In order to generate hypotheses on the diets of siphonophores using tentilla morphology,
119 we used the discriminant analyses of principal components (DAPC) (Jombart et al. 2010)
120 trained in Damian-Serrano et al. (2020). We predict the feeding guilds of species in the
121 dataset for which there are no published feeding observations using their morphological data
122 as inputs, and presenting the predictive output in the form of posterior probabilities for each

¹²³ guild category.

¹²⁴ In order to observe the discharge behavior of different tentilla, we recorded high speed
¹²⁵ footage (1000-3000 fps) of tentillum and nematocyst discharge by live siphonophore specimens
¹²⁶ (26 species) using a Phantom Miro 320S camera mounted on a stereoscopic microscope. We
¹²⁷ mechanically elicited tentillum and nematocyst discharge using a fine metallic pin. We used
¹²⁸ the Phantom PCC software to analyze the footage. For the 10 species recorded, we measured
¹²⁹ total cnidoband discharge time (ms), heteroneme filament length (μm), and discharge speeds
¹³⁰ (mm/s) for cnidoband, heteronemes, haplonemes, and heteroneme shafts when possible (data
¹³¹ available in the Supplementary Information).

¹³² Results

¹³³ *Evolutionary history of tentillum morphology* – In Damian-Serrano et al. (2020), we produced
¹³⁴ the most speciose siphonophore molecular phylogeny to date, while incorporating the most
¹³⁵ recent findings in siphonophore deep node relationships. This phylogeny revealed for the first
¹³⁶ time that the genus *Erenna* is the sister to *Stephanomia amphytridis*. *Erenna* and *Stephanomia*
¹³⁷ bear the largest tentilla among all siphonophores, thus their monophyly indicates that there
¹³⁸ was a single evolutionary transition to giant tentilla. Siphonophore tentilla range in size
¹³⁹ from $\sim 30 \mu\text{m}$ in some *Cordagalma* specimens to 2-4 cm in *Erenna* species, and up to 8 cm
¹⁴⁰ in *Stephanomia amphytridis* (Pugh and Baxter 2014). Most siphonophore tentilla measure
¹⁴¹ between 175 and 1007 μm (1st and 3rd quartiles), with a median of 373 μm . The extreme
¹⁴² gain of tentillum size in this newly found clade may have important implications for access
¹⁴³ to large prey size classes such as adult deep-sea fishes.

¹⁴⁴ Siphonophore tentilla are defined as lateral, monostichous evaginations of the tentacle (in-
¹⁴⁵ cluding its gastrovascular lumen), armed with epidermal nematocysts (Totton and Bargmann
¹⁴⁶ 1965). The buttons on *Physalia* tentacles were not traditionally regarded as tentilla, but
¹⁴⁷ Bardi and Marques (2007), Munro et al. (2018), and our own observations confirm that
¹⁴⁸ the buttons contain evaginations of the gastrovascular lumen, thus satisfying all the criteria

for the definition. In this light, and given that most Cystonectae bear conspicuous tentilla, we conclude (in agreement with Munro et al. (2018) and Damian-Serrano et al. (2020)) that tentilla were present in the most recent common ancestor of all siphonophores, and secondarily lost twice, once in *Apolemia* and again in *Bathyphysa conifera*. In order to gain a broad perspective on the evolutionary history of tentilla, we reconstructed the phylogenetic positions of the main categorical character shifts (such as gains and losses of nematocyst types) using stochastic character mapping (SM1-9) and manual reconstructions. This phylogenetic roadmap of evolutionary novelties is summarized in (Fig. 4).

We assume that haploneme nematocysts are ancestrally present in siphonophore tentacles since they are present in the tentacles of many other hydrozoans (Mariscal 1974). Haplonemes are toxin-bearing open-ended nematocysts characterized by the lack of a shaft preceding the tubule. Two subtypes are found in siphonophores: the isorhizas of homogeneous tubule width, and the anisorhizas with a slight bulking of the tubule near the base. In Cystonectae, haplonemes diverged into spherical isorhizas of two size classes. There is one size of haplonemes in Codonophora, which consist of elongated anisorhizas. Haplonemes were likely lost in the tentacles of *Apolemia* but retained as spherical isorhizas in other *Apolemia* tissues (Siebert et al. 2013). While heteronemes exist in other tissues of cystonects, they appear in the tentacles of codonophorans exclusively, as birhopaloids in *Apolemia*, stenoteles in eucladophoran physonects, and microbasic mastigophores in calycothorans. The four nematocyst types unique to siphonophores appear in two events in the phylogeny (Fig. 4): birhopaloids arose in the stem to *Apolemia*, while rhopalonemes (acrophore and anacrophore) and homotrichous anisorhizas arose in the stem to Tendiculophora.

Nematocyst type gain and loss is also associated with prey capture functions. For example, the loss of desmonemes and rhopalonemes in piscivorous *Erenna*, retaining solely the penetrant (and venom injecting) anisothizas and stenoteles (two size classes) is reminiscent of the two size classes of penetrant isorhizas in the fish-specialist cystonects. Moreover, with the gain of anisorhizas, desmonemes, and rhopalonemes, the Tendiculophora gained versatility in

176 entangling and adhesive functions of the cnidoband and terminal filament, which may have
177 allowed their feeding niches to diversify. Part of the effectiveness of calycophoran cnidobands
178 at entangling crustaceans may be attributed to the subspecialization of their heteronemes.
179 These shifted from the ancestral penetrating stenotele to the microbasic mastigophore (or
180 eurytele in some species) with a long barbed shaft armed with many long spines. This
181 heteroneme subtype could be better at interlocking with the setae of crustacean legs and
182 antennae.

183 In those species that have a functional terminal filament, the desmonemes and
184 rhopalonemes play a fundamental role in the first stages of adhesion of the prey. In many
185 species, the tugs of the struggling prey on the terminal filament trigger the cnidoband
186 discharge (Mackie et al. 1987 and pers. obs.). The adhesive terminal filament has been
187 lost several times in the Euphysonectae (*Frillagalma*, *Lychnagalma-Physophora*, *Erenna*,
188 and some species of *Cordagalma*). In these species, we hypothesize that a different trigger
189 mechanism is at play, possibly involving the prey actively biting or grasping the tentillum or
190 lure.

191 The clades defined in Damian-Serrano et al. (2020) are characterized by unique evolu-
192 tionary innovations in their tentilla. The clade Eucladophora (containing Pyrostephidae,
193 Euphysonectae, and Calycophorae) encompasses all of the extant Siphonophore species (178
194 of 186) except Cystonects and *Apolemia*. Innovations that arose along the stem of this group
195 include spatially segregated heteroneme and haploneme nematocysts, terminal filaments, and
196 elastic strands (Fig. 4). Pyrostephids evolved a unique bifurcation of the axial gastrovascular
197 canal of the tentillum known as the “saccus” (Totton and Bargmann 1965). The stem to
198 the clade Tendiculophora (clade containing Euphysonectae and Calycophorae) subsequently
199 acquired further novelties such as the desmoneme and rhopaloneme (acrophore subtype
200 ancestral) nematocysts on the terminal filament (Fig. 4), which bears no other nematocyst
201 type. These are arranged in sets of 2 parallel rhopalonemes for each single desmoneme (Skaer
202 1988, 1991). The involucrum is an expansion of the epidermal layer that can cover part or

²⁰³ all of the cnidoband (Fig. 2). This structure, together with differentiated larval tentilla,
²⁰⁴ appeared in the stem branch to Clade A physonects. Calycophorans evolved novelties such as
²⁰⁵ larger desmonemes at the distal end of the cnidoband, pleated pedicles with a “hood” (here
²⁰⁶ considered homologous to the involucrum) at the proximal end of the tentillum, anacrophore
²⁰⁷ rhopalonemes, and microbasic mastigophore-type heteronemes. While calycophorans have
²⁰⁸ diversified into most of the extant described siphonophore species (108 of 186), their tentilla
²⁰⁹ have not undergone any major categorical gains or losses since their most recent common
²¹⁰ ancestor. Nonetheless, they have evolved a wide variation in nematocyst and cnidoband
²¹¹ sizes. Ancestrally (and retained in most prayomorphs and hippopodids), the calycophoran
²¹² tentillum is recurved where the proximal and distal ends of the cnidoband are close together.
²¹³ Diphyomorph tentilla are slightly different in shape, with straighter cnidobands.

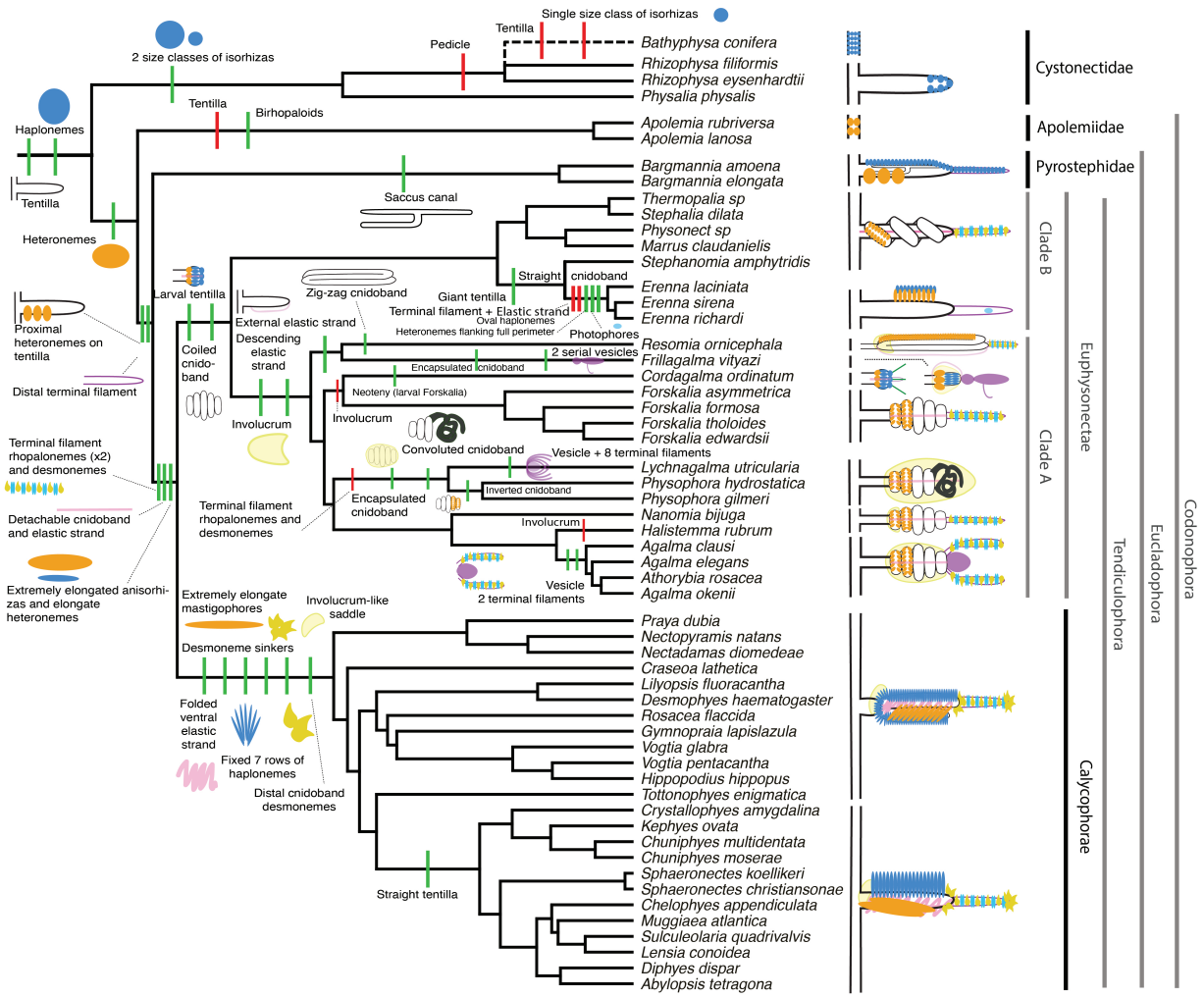


Figure 4: Siphonophore cladogram with the main categorical character gains (green) and losses (red) mapped. Some branch lengths were modified from the Bayesian chronogram to improve readability. The main visually distinguishable tentillum types are sketched next to the species that bear them, showing the location and arrangement of the main characters. In large, complex-shaped euphysonect tentilla, haplonemes were omitted for simplification. The hypothesized phylogenetic placement of the rhizophysid *Bathyphysa conifera*, for which no molecular data are yet available, was added manually (dashed line).

214 *Evolution of tentillum and nematocyst characters* – Most (74%) characters present a
215 significant phylogenetic signal, yet only total nematocyst volume, haploneme length, and
216 heteroneme-to-cnidoband length ratio had a phylogenetic signal with K larger than 1 (SM10).
217 Total nematocyst volume and cnidoband-to-heteroneme length ratio showed strongly conserved
218 phylogenetic signals. The majority (67%) of characters were best fitted by BM models,
219 indicating a history of neutral constant divergence. We did not find any relationship
220 between phylogenetic signal and specific model support, where characters with high and low
221 phylogenetic signal were broadly distributed among the best fitted for each model. One-third
222 of the characters measured in Damian-Serrano et al. (2020) did not recover significant support
223 for any of the phylogenetic models tested, indicating they are either not phylogenetically
224 conserved, or they evolved under a complex evolutionary process not represented among the
225 models tested (SM10). Haploneme nematocyst length was the only character with support
226 for an EB model of decreasing rate of evolution with time. No character had support for a
227 single-optimum OU model (when not informed by feeding guild regime priors). The model
228 adequacy tests (SM11) indicate that many characters may have a relationship between the
229 states and the rates of evolution (Sasr) not captured in the basic models compared here,
230 accompanied by a signal of unaccounted rate heterogeneity (Cvar). No characters show
231 significant deviations in the overall rate of evolution estimated (Msig). Some characters
232 show a perfect fit (no significant deviations across all metrics) under BM evolution, such as
233 heteroneme shape, length, width & volume, haploneme width & SA/V, tentacle width and
234 pedicle width. Haploneme row number and rhopaloneme shape have significant deviations
235 across four metrics, indicating that BM (best model) is a poor fit. These characters likely
236 evolved under complex models which would require many more data points than we have
237 available to fit with accuracy.

238 *Phenotypic integration of the tentillum* – Phenotypically integrated structures maintain
239 evolutionary correlations between its constituent characters. Of the phylogenetic correlations
240 among tentillum and nematocyst characters examined here (Fig. 5a, lower triangle), 81.3%

were positive and 18.7% were negative, while of the ordinary correlations (Fig. 5a, upper triangle) 74.6% were positive and 25.4% were negative. Half (49.9%) of phylogenetic correlations were >0.5 , while only 3.6% are < -0.5 . Similarly, among the correlations across extant species, 49.1% were >0.5 and only 1.5% were < -0.5 . In addition, we found that 13.9% of character pairs had opposing phylogenetic and ordinary correlation coefficients (Fig. 5B). Just 4% of character pairs have negative phylogenetic and positive ordinary correlations (such as rhopaloneme elongation \sim heteroneme-to-cnidoband length ratio and haploneme elongation, or haploneme elongation \sim heteroneme number), and only 9.9% of character pairs had positive phylogenetic correlation yet negative ordinary correlation (such as heteroneme elongation \sim cnidoband convolution and involucrum length, or rhopaloneme elongation with cnidoband length). These disparities could be explained by Simpson's paradox (Blyth 1972): the reversal of the sign of a relationship when a third variable (or a phylogenetic topology, as suggested by Uyeda et al. (2018)) is considered. However, no character pair had correlation coefficient differences larger than 0.64 between ordinary and phylogenetic correlations (heteroneme shaft extension \sim rhopaloneme elongation has a Pearson's correlation of 0.10 and a phylogenetic correlation of -0.54). Rhopaloneme elongation shows the most incongruencies between phylogenetic and ordinary correlations with other characters. We identified four hypothetical modules among the tentillum characters: (1) The tentillum scaffold module including cnidoband length & width, nematocyst row number, pedicle & elastic strand width, tentacle width; (2) the heteroneme module including heteroneme length & width, shafts length & width; (3) the haploneme module including length and width; and (4) the terminal filament module including desmoneme & rhopaloneme length & width. The phenotypic integration test showed significant integration signal between all modules, tentillum and haploneme modules sharing the greatest regression coefficient (SM12).

Evolution of nematocyst shape – The greatest evolutionary change in haploneme nematocyst shape occurred in a single shift towards elongation in the stem of Tendiculophora, which contains the majority of described siphonophore species, *i.e.* all siphonophores other

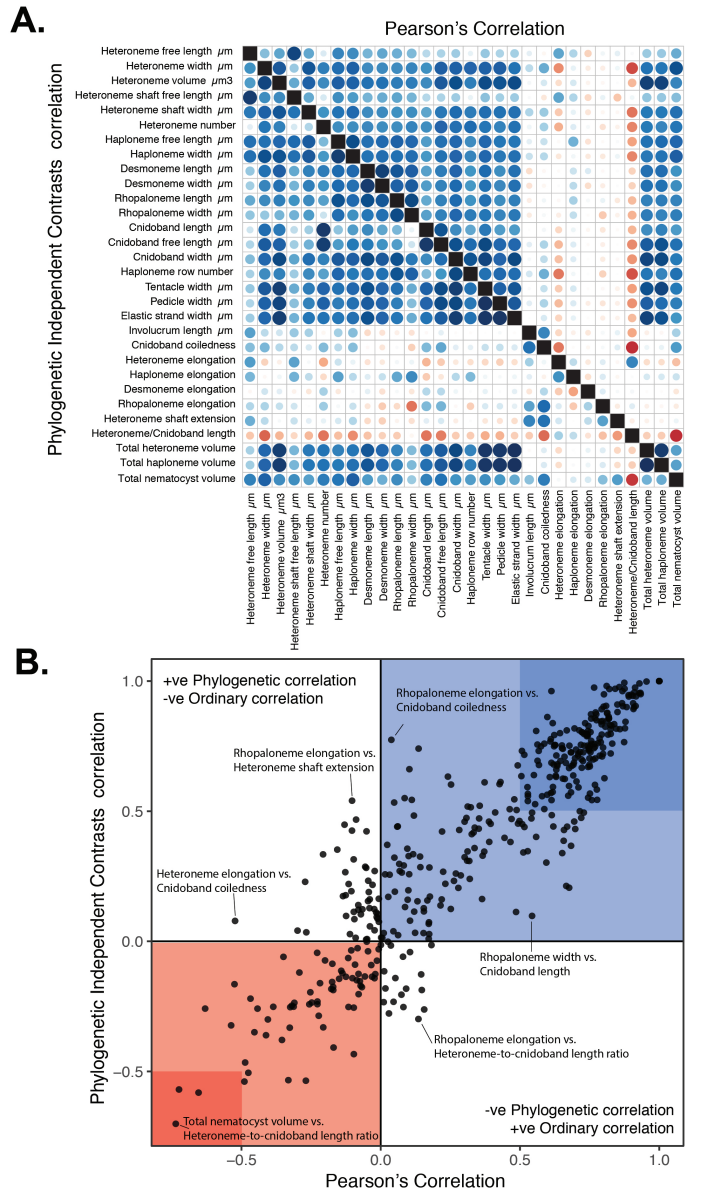


Figure 5: A. Correlogram showing strength of ordinary (upper triangle) and phylogenetic (lower triangle) correlations between characters. Both size and color of the circles indicate the strength of the correlation (R^2). B. Scatterplot of phylogenetic correlation against ordinary correlation showing a strong linear relationship ($R^2 = 0.92$, 95% confidence between 0.90 and 0.93). Light red and blue boxes indicate congruent negative and positive correlations respectively. Darker red and blue boxes indicate strong (<-0.5 or >0.5) negative and positive correlation coefficients respectively.

²⁶⁸ than Cystonects, *Apolemia*, and Pyrostephidae. There is one secondary return to more
²⁶⁹ oval, less elongated haplonemes in *Erenna*, but it does not reach the sphericity present
²⁷⁰ in Cystonectae or Pyrostephidae (Fig. 6). Heteroneme evolution presents a less discrete
²⁷¹ evolutionary history. Tendiculophora evolved more elongate heteronemes along the stem, but
²⁷² the difference between theirs and other siphonophores' is much smaller than the variation
²⁷³ in shape within Tendiculophora, bearing no phylogenetic signal within this clade. In this
²⁷⁴ clade, the evolution of heteroneme shape has diverged in both directions, and there is no
²⁷⁵ correlation with haploneme shape (Fig. 6), which has remained fairly constant (elongation
²⁷⁶ between 1.5 and 2.5).

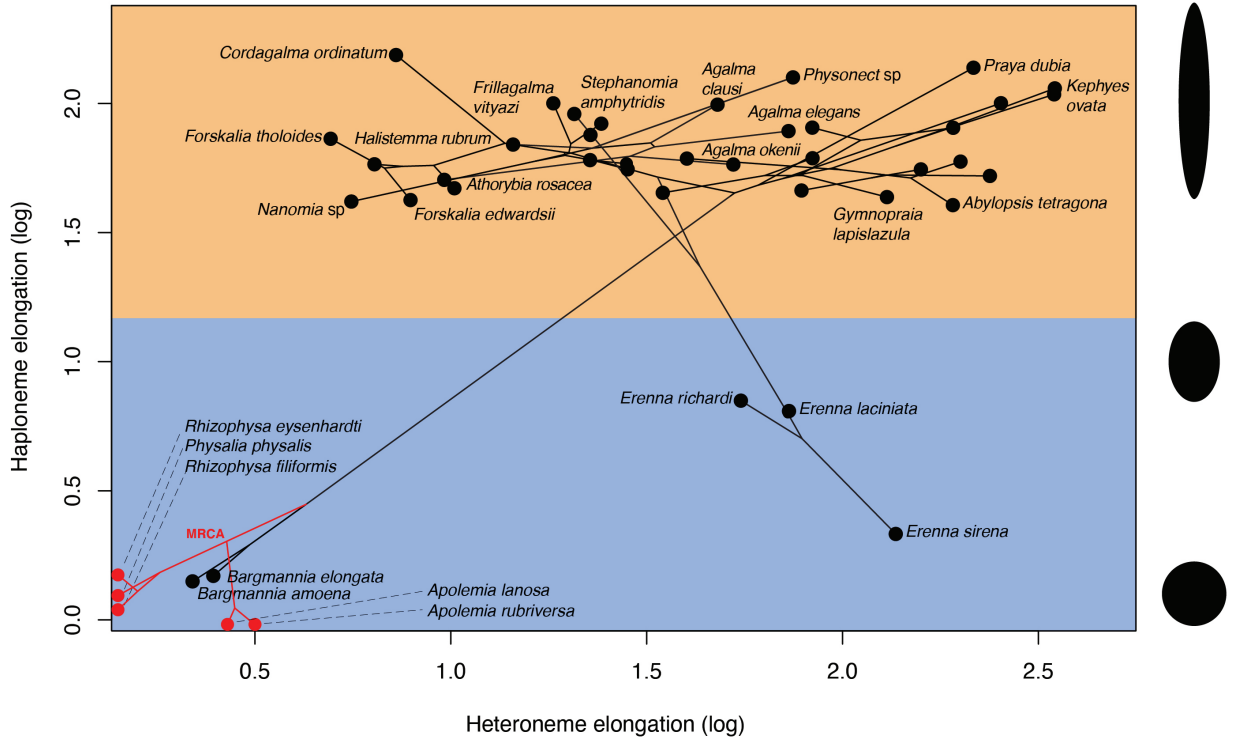


Figure 6: Phylomorphospace showing haploneme and heteroneme elongation (log scaled). Orange area delimits rod-shaped haplonemes, the blue area covers oval and round-shaped haplonemes. Smaller dots and lines represent phylogenetic relationships and ancestral states of internal nodes under BM. Species nodes in red lack either haplonemes or heteronemes, and their values are projected onto the axis of the nematocyst type they bear. Cystonects have no tentacle heteronemes and are projected onto the haploneme axis. Apolemiids have no tentacle haplonemes and are projected onto the heteroneme axis.

²⁷⁷ Haploneme and heteroneme shape share 21% of their variance across extant values, and
²⁷⁸ 53% of the variance in their shifts along the branches of the phylogeny. However, much of
²⁷⁹ this correlation is due to the sharp contrast between Pyrostephidae and their sister group
²⁸⁰ Tendiculophora. We searched for regime shifts in the evolution of haploneme nematocyst
²⁸¹ shape characters using SURFACE (Ingram and Mahler 2013). SURFACE identified eight
²⁸² distinct OU regimes in the evolutionary history of haploneme length and width (Fig. 7A).
²⁸³ The different regimes are located (1) in cystonects, (2) in most of Tendiculophora, (3) in
²⁸⁴ most diphyomorphs, (4) in *Cordagalma ordinatum*, (5) in *Stephanomia amphytridis*, (6) in
²⁸⁵ pyrostephids, (7) in *Diphyes dispar* + *Abylopsis tetragona*, and (8) in *Erenna* spp.

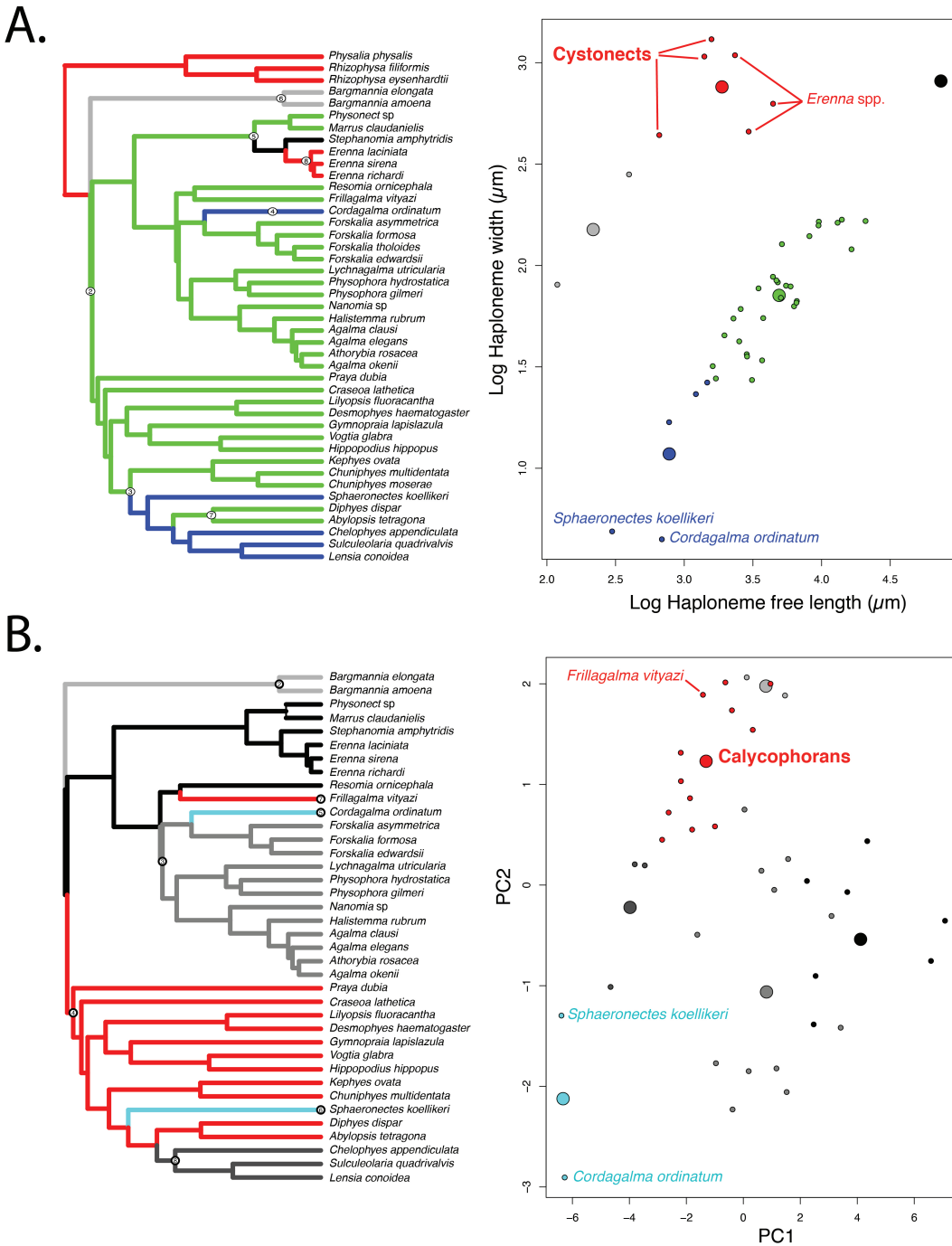


Figure 7: SURFACE plots showing convergent evolutionary regimes modelled under OU for (A) haploneme nematocyst length & width, and (B) for PC1 & PC2 of all continuous characters with the exception of terminal filament nematocysts, and removing taxa with inapplicable character states. Node numbers on the tree label different regimes, regimes of the same color are identified as convergent. Small circles on the scatterplots indicate species values, large circles indicate the average position of the OU optima (θ) for a given combination of convergent regimes.

²⁸⁶ In the non-phylogenetic PCA morphospace using only characters derived from simple
²⁸⁷ measurements (Fig. 8), PC1 (aligned with tentillum and tentacle size) explained 69.3% of
²⁸⁸ the variation in the tentillum morphospace, whereas PC2 (aligned with heteroneme length,
²⁸⁹ heteroneme number, and haploneme arrangement) explained 13.5%. In a phylogenetic PCA,
²⁹⁰ 63% of the evolutionary variation in the morphospace is explained by PC1 (aligned with
²⁹¹ shifts in tentillum size), while 18% is explained by PC2 (aligned with shifts in heteroneme
²⁹² number and involucrum length).

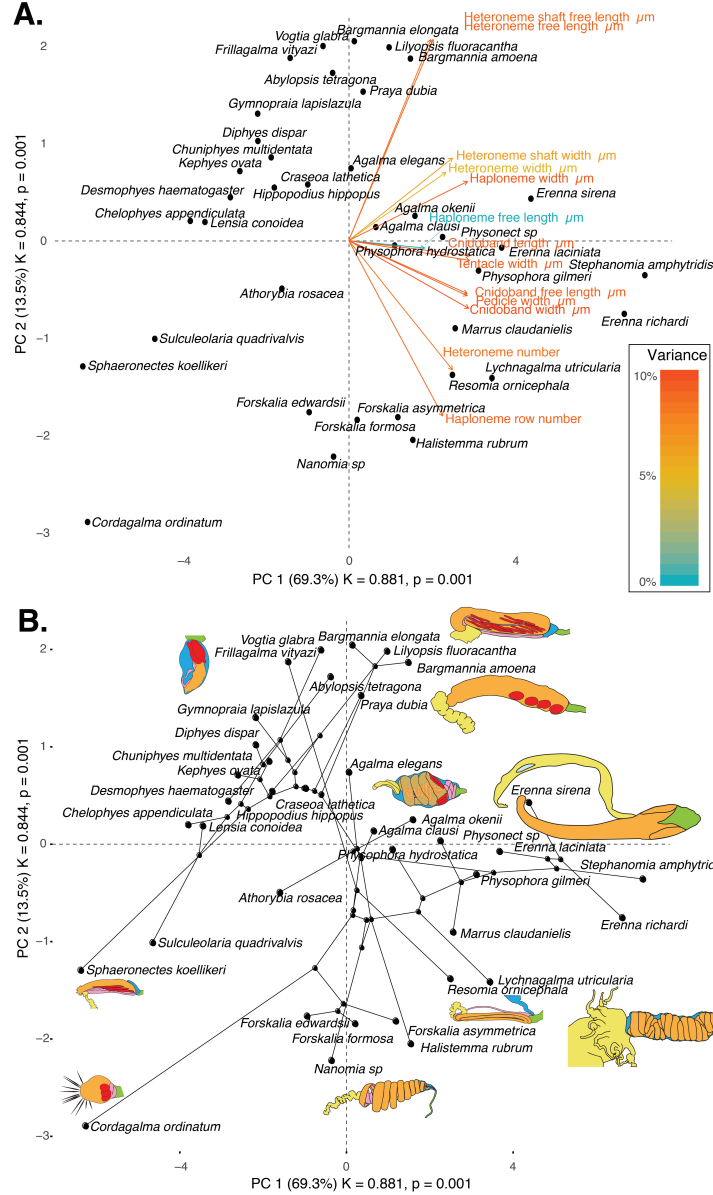


Figure 8: PCA of the simple-measurement continuous characters principal components, excluding ratios and composite characters. A. Variance explained by each variable in the PC1-PC2 plane. Axis labels include the phylogenetic signal (K) for each component and p-value. B. Phylogenetic relationships between the species points and reconstructed ancestors distributed in that same space.

293 *Morphospace occupation* – In order to examine the occupation structure of the morphospace
294 across all siphonophore species in the dataset, we cast a PCA on the data after transforming
295 inapplicable states (due to absence of character) to zeroes. This allows us to accommodate
296 species with many missing characters (such as cystonects or apolemiids), and to account
297 for common absences as morphological similarities. In this ordination, PC1 (aligned with
298 cnidoband size) explains 47.45% of variation and PC2 (aligned with heteroneme volume
299 and involucrum length) explains 16.73% of variation. When superimposing feeding guilds
300 onto the morphospace (Fig. 9), we find that the morphospaces of each feeding guild are
301 only slightly overlapping in PC1 and PC2. A phylogenetic MANOVA showed that feeding
302 guilds explain 27.63% of variance across extant species (p value < 0.000001), and 20.97%
303 of the variance when accounting for phylogeny, an outcome significantly distinct from the
304 expectation under neutral evolution (p -value = 0.0196). In addition, a morphological disparity
305 analysis accounting for phylogenetic structure shows that the morphospace of fish specialists
306 is significantly broader than that of generalists and other specialists. This is due to the large
307 morphological disparities between cystonects and piscivorous euphysonects. There are no
308 significant differences among the morphospace disparities of the other feeding guilds.

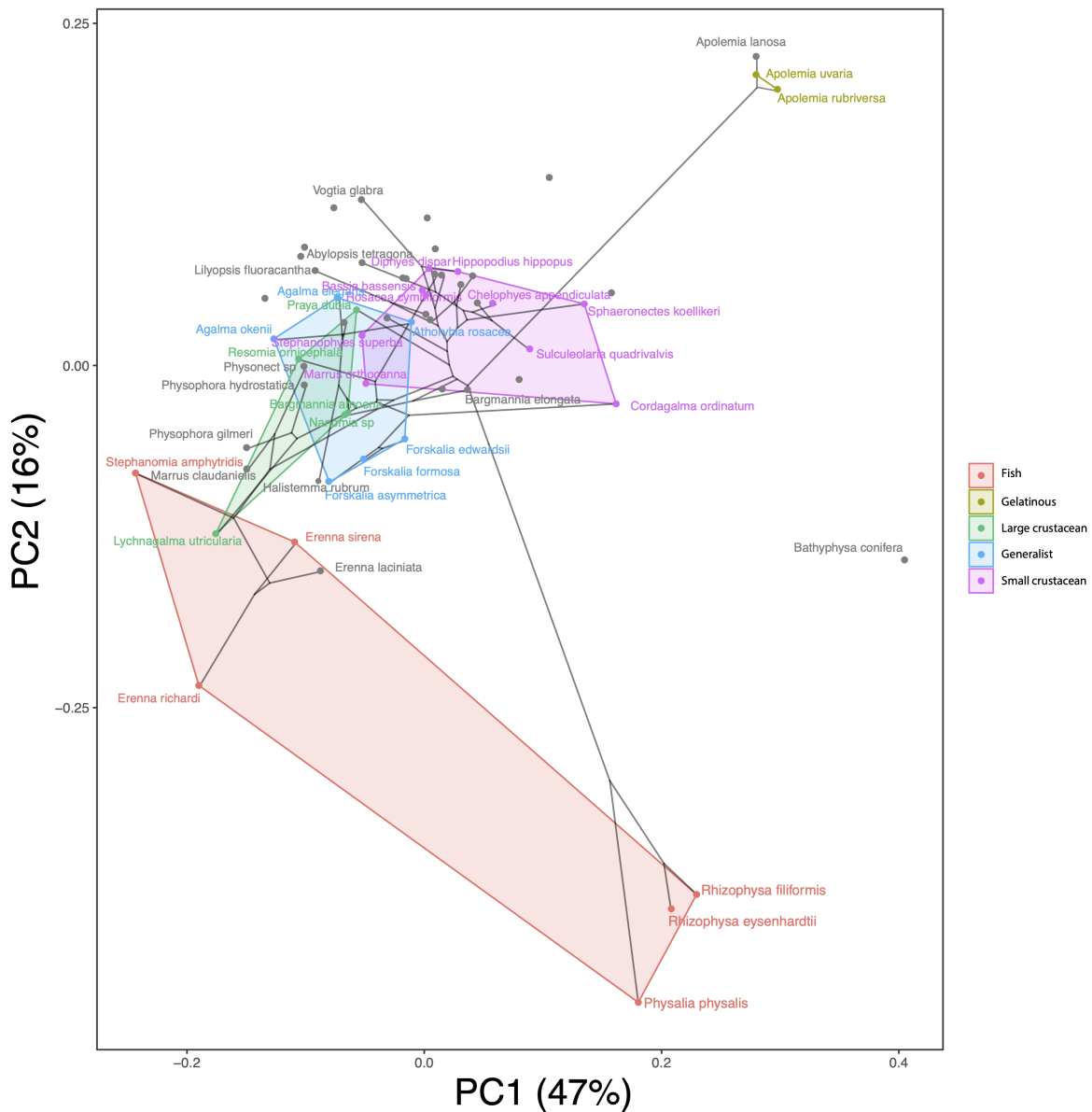


Figure 9: Phylomorphospace showing PC1 and PC2 from a PCA of continuous morphological characters with inapplicable states transformed to zeroes, overlapped with polygons conservatively defining the space occupied by each feeding guild. Lines between species coordinates show the phylogenetic relationships between them.

309 *Convergent evolution* – Convergence is a widespread evolutionary phenomenon where
310 distantly related clades independently evolve similar phenotypes. When the dimensionality
311 of the state space is small as it is in tentilla morphology, convergence is more likely given the
312 same amount of evolutionary change. Using the package SURFACE (Ingram and Mahler
313 2013), we identified convergence in haploneme nematocyst shape and in morphospace position.
314 In Damian-Serrano et al. (2020), we identified haploneme nematocyst shape as one of the
315 traits associated with the convergent evolution of piscivory. Here we find that indeed wider
316 haploneme nematocysts have convergently evolved in the piscivore cytonects and *Erenna*
317 spp. (Fig. 7A). Extremely narrow haplonemes have also evolved convergently in *Cordagalma*
318 *ordinatum* and copepod specialist calycophorans such as *Sphaeronectes koellikeri*. When
319 integrating many traits into a couple principal components, we find two distinct convergences
320 between euphysonects and calycophorans with a reduced prey capture apparatus. Those
321 convergences are between *Frillagalma vityazi* and calycophorans, and once again between
322 *Cordagalma ordinatum* and *Sphaeronectes koellikeri* (Fig. 7B).

323 *Functional morphology of tentillum and nematocyst discharge* – Tentillum and nematocyst
324 discharge high speed videos and measurements are available in the Supplementary Information.
325 While the sample sizes of these measurements were insufficient to draw reliable statistical
326 results at a phylogenetic level, we did observe patterns that may be relevant to their functional
327 morphology. For example, cnidoband length is strongly correlated with discharge speed (p
328 value = 0.0002). This explains much of the considerable difference between euphysonect and
329 calycophoran tentilla discharge speeds (average discharge speeds: 225.0mm/s and 41.8mm/s
330 respectively; t-test p value = 0.011), since the euphysonects have larger tentilla than the
331 calycophorans among the species recorded. In addition, we observed that calycophoran
332 haploneme tubules fire faster than those of euphysonects (t-test p value = 0.001). Haploneme
333 nematocysts discharge 2.8x faster than heteroneme nematocysts (t-test p value = 0.0012).
334 Finally, we observed that the stenoteles of the Euphysonectae discharge a helical filament
335 that “drills” itself through the medium it penetrates as it everts.

Generating dietary hypotheses using tentillum morphology – For many siphonophore species, no feeding observations have yet been published. To help bridge this gap of knowledge, we generated hypotheses about the diets of these understudied siphonophores (Fig. 10) based on their known tentacle morphology using one of the linear discriminant analyses of principal components (DAPC) fitted in Damian-Serrano et al. (2020). This provides concrete predictions to be tested in future work and helps extrapolate our findings to many poorly known species that are extremely difficult to collect and observe. The discriminant analysis for feeding guild (7 principal components, 4 discriminants) produced 100% discrimination, and the highest loading contributions were found for the characters (ordered from highest to lowest): Involucrum length, heteroneme volume, heteroneme number, total heteroneme volume, tentacle width, heteroneme length, total nematocyst volume, and heteroneme width. We used the predictions from this discriminant function to generate hypotheses about the feeding guild of 45 species in the morphological dataset. This extrapolation predicts that two other *Apolemia* species are gelatinous prey specialists like *Apolemia rubriversa*, and predicts that *Erenna laciniata* is a fish specialist like *Erenna richardi*. When predicting soft- and hard-bodied prey specialization, the DAPC achieved 90.9% discrimination success, only marginally confounding hard-bodied specialists with generalists (SM13). The main characters driving this discrimination are involucrum length, heteroneme number, heteroneme volume, tentacle width, total nematocyst volume, total haploneme volume, elastic strand width, and heteroneme length.

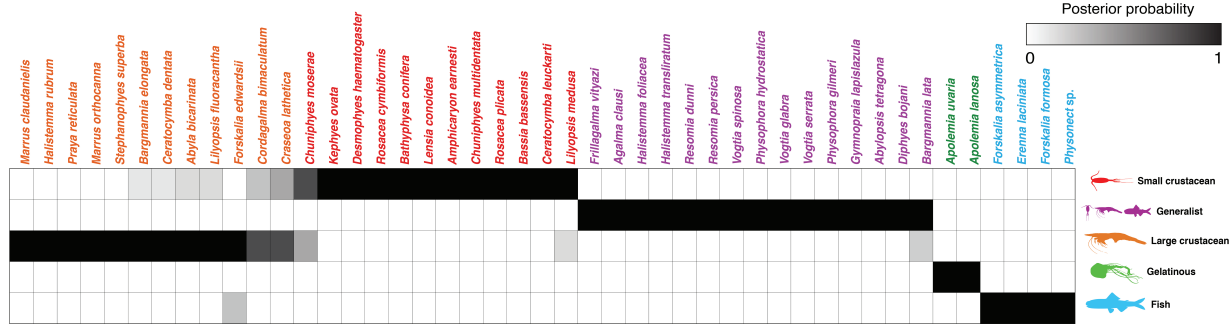


Figure 10: Hypothetical feeding guilds for siphonophore species predicted by a 6 PCA DAPC. Cell darkness indicates the posterior probability of belonging to each guild. The training dataset was transformed so inapplicable states are computed as zeroes. Species are sorted and colored according to their predicted feeding guild.

356 Discussion

357 *On the evolution of tentilla morphology* – The evolutionary history of siphonophore tentilla
 358 shows three major transition points which have structured the morphological diversity we
 359 see today. First, the earliest split between codonophorans and cystonects divides lineages
 360 with penetrating isorhizas from those which utilize heteronemes for prey capture. Second,
 361 the split between apolemiids and eucladophorans divided the simple-tentacled *Apolemia* from
 362 the lineage that evolved composite tentilla with heteronemes and haplonemes. Finally, the
 363 branch leading to tendiculophorans fostered innovations such as the elastic strands and the
 364 terminal filament nematocysts which produced the most complex tentilla structures and
 365 greatest morphological diversity we observe among siphonophores.

366 Siphonophore tentilla are beautifully complex and highly diverse. Our new analyses
 367 show, however, that the siphonophore tentillum morphospace actually has a fairly low extant
 368 dimensionality due to having an evolutionary history with many synchronous, correlated
 369 changes. This can be due to many causes including structural constraints, developmental
 370 constraints, or selection that reduces the viable state space. Though siphonophore development
 371 has not been extensively studied, what is known suggests that developmental constraints alone
 372 could not explain the highly correlated evolutionary changes we observe. The nematocysts
 373 that arm the tentillum are developed in a completely separate region of the gastrozooid

³⁷⁴ (Carré 1972) and then migrate and assemble within the tentillum later on (Skaer 1988).
³⁷⁵ This lack of proximity and physical independence of development between traits makes
³⁷⁶ developmental constraints unlikely. Surprisingly, many of the strong correlations we find
³⁷⁷ are between nematocyst and structural tentillum characters. Therefore, we hypothesize the
³⁷⁸ genetic correlations and phenotypic integration between tentillum and nematocyst characters
³⁷⁹ are maintained through natural selection on separate regulatory networks, out of the necessity
³⁸⁰ to work together and meet the spatial, mechanical, and functional constraints of their prey
³⁸¹ capture behavior. In order to adequately test these hypotheses, future work would need to
³⁸² study the genetic mechanisms underlying the development of tentilla from a comparative,
³⁸³ evolutionary approach. Fortunately, the unique biology of siphonophore tentacles displays
³⁸⁴ the full developmental sequence of tentilla along each tentacle, making siphonophores an
³⁸⁵ ideal system for the comparative study of development.

³⁸⁶ In Damian-Serrano et al. (2020) we examined the covariance terms in the multivariate rate
³⁸⁷ matrix for the evolution of tentillum and nematocyst characters. Building on this work, here
³⁸⁸ we examine the correlations among the trait values while accounting for phylogenetic structure.
³⁸⁹ The results for both analyses indicate that tentilla are not only phenotypically integrated (with
³⁹⁰ widespread evolutionary correlations across structures) but also show patterns of evolutionary
³⁹¹ modularity, where different sets of characters appear to evolve in stronger correlations
³⁹² among each other than with other characters (Wagner 1996). This may be indicative of the
³⁹³ underlying genetic and developmental dependencies among closely homologous nematocyst
³⁹⁴ types (such as desmonemes and rhopalonemes) and structures. In addition, these evolutionary
³⁹⁵ modules point to hypothetical functional modules. For example, the coiling degree of the
³⁹⁶ cnidoband and the extent of the involucrum have correlated rates of evolution, while the
³⁹⁷ involucrum may help direct the whiplash of the uncoiling cnidoband distally (towards the
³⁹⁸ prey). The evolutionary innovation of the Tendiculophora tentilla with shooting cnidobands
³⁹⁹ and modular regions may have facilitated further dietary diversification. A specific instance
⁴⁰⁰ of this dietary diversification may have been the access to the abundant small crustacean

401 prey such as copepods. The rapid darting escape response of copepods may preclude their
402 capture in siphonophores without shooting cnidobands. The trophic opportunities unlocked
403 by these morphological novelties may be responsible for the far greater number of species in
404 Tendicilophora than its relatives Cystonectae, Apolemiidae, and Pyrostephidae.

405 *Heterochrony and convergence in the evolution of tentilla with diet* - In addition to identi-
406 fying shifts in prey type, Damian-Serrano et al. (2020) revealed the specific morphological
407 changes in the prey capture apparatus associated with these shifts. Copepod-specialized
408 diets have evolved independently in *Cordagalma* and some calycophorans. These evolutionary
409 transitions happened together with transitions to smaller tentilla with fewer and smaller
410 cnidoband nematocysts. We found that these morphological transitions evolved convergently
411 in these taxa. Tentilla are expensive single-use structures (Mackie et al. 1987), therefore we
412 would expect that specialization in small prey would beget reductions in the size of the prey
413 capture apparatus to the minimum required for the ecological performance. Such a reduction
414 in size would require extremely fast rates of trait evolution in an ordinary scenario. However,
415 *Cordagalma*'s tentilla strongly resemble the larval tentilla (only found in the first-budded
416 feeding body of the colony) of their sister genus *Forskalia*. This indicates that the evolution of
417 *Cordagalma* tentilla could be a case of paedomorphic heterochrony associated with predatory
418 specialization on smaller prey. This developmental shift may have provided a shortcut for
419 the evolution of a smaller prey capture apparatus.

420 Our work identifies yet another novel example of convergent evolution. The region of the
421 tentillum morphospace occupied by calycophorans was independently (and more recently)
422 occupied by the physonect *Frillagalma vityazi* (Fig. 7B). Like calycophorans, *Frillagalma*
423 tentilla have small C-shaped cnidobands with a few rows of anisorhizas. Unlike calycophorans,
424 they lack paired elongate microbasic mastigophores. Instead, they bear exactly three oval
425 stenoteles, and their cnidobands are followed by a branched vesicle, unique to this genus.
426 Their tentillum morphology is very different from that of other related physonects, which tend
427 to have long, coiled, cnidobands with many paired oval stenoteles. Our SURFACE analysis

428 clearly indicates a regime convergence in the cnidoband morphospace between *Frillagalma* and
429 calycophorans (Fig. 7B). Most studies on calycophoran diets have reported their prey to be
430 primarily composed of small crustaceans, such as copepods or ostracods (Purcell 1981, 1984).
431 The diet of *Frillagalma vityazi* is unknown, but this morphological convergence suggests that
432 they evolved to capture similar kinds of prey. However, our DAPCs predict that *Frillagalma*
433 has a generalist niche (Fig. 10) with both soft and hard-bodied prey (SM13).

434 *Evolution of nematocyst shape* – A remarkable feature of siphonophore haplonemes is
435 that they are outliers to all other Medusozoa in their surface area to volume relationships,
436 deviating significantly from sphericity (Thomason 1988). This suggests a different mechanism
437 for their discharge that could be more reliant on capsule tension than on osmotic potentials
438 (Carré and Carré 1980), and strong selection for efficient nematocyst packing in the cnidoband
439 (Skaer 1988; Thomason 1988). Our results show that Codonophora underwent a shift towards
440 elongation and Cystonectae towards sphericity, assuming the common ancestor had an
441 intermediate state. Since we know that the haplonemes of other hydrozoan outgroups are
442 generally spheroid, it is more parsimonious to assume that cystonects are simply retaining
443 this ancestral state. Later, we observe a return to more rounded (ancestral) haplonemes in
444 *Erenna*, concurrent with a secondary gain of a piscivorous trophic niche, like that exhibited
445 by cystonects. Our SURFACE analysis shows that this transition to roundness is convergent
446 with the regime occupied by cystonects (Fig. 7A). Purcell (1984) showed that haplonemes
447 have a penetrating function as isorhizas in cystonects and an adhesive function as anisorhizas
448 in Tendiculophora. It is no coincidence that the two clades that have converged to feed
449 primarily on fish have also converged morphologically toward more compact haplonemes.
450 Isorhizas in cystonects are known to penetrate the skin of fish during prey capture, and to
451 deliver the toxins that aid in paralysis and digestion (Hessinger 1988). *Erenna*'s anisorhizas
452 are also able to penetrate human skin and deliver a painful sting (Pugh 2001), a common
453 feature of piscivorous cnidarians like the Portuguese man-o-war or box jellies.

454 The implications of these results for the evolution of nematocyst function are that

455 an innovation in the discharge mechanism of haplonemes may have occurred during the
456 main shift to elongation. Elongate nematocysts can be tightly packed into cnidobands.
457 We hypothesize this may be a Tendiculophora lineage-specific adaptation to packing more
458 nematocysts into a limited tentillum space, as suggested by (Skaer 1988). Thomason (1988)
459 hypothesized that smaller, more spherical nematocysts, with a lower surface area to volume
460 ratio, are more efficient in osmotic-driven discharge and thus have more power for skin
461 penetration. The elongated haplonemes of crustacean-eating Tendiculophora have never
462 been observed penetrating their crustacean prey (Purcell 1984), and are hypothesized to
463 entangle the prey through adhesion of the abundant spines to the exoskeletal surfaces
464 and appendages. Entangling requires less acceleration and power during discharge than
465 penetration, as it does not rely on point pressure. In fish-eating cystonects and *Erenna* species,
466 the haplonemes are much less elongated and very effective at penetration, in congruence with
467 the osmotic discharge hypothesis. Tendiculophora, composed of the clades Euphysonectae
468 and Calycophorae, includes the majority of siphonophore species. Within these clades are the
469 most abundant siphonophore species, and a greater morphological and ecological diversity is
470 found. We hypothesize that this packing-efficient haploneme morphology may have also been
471 a key innovation leading to the diversification of this clade. However, other characters that
472 shifted concurrently in the stem of this clade could have been equally responsible for their
473 extant diversity.

474 *Generating hypotheses on siphonophore feeding ecology* – One motivation for our research
475 is to understand the links between prey-capture tools and diets so we can generate hypotheses
476 about the diets of predators based on morphological characteristics. Indeed, our discriminant
477 analyses were able to distinguish between different siphonophore diets based on morphological
478 characters alone. The models produced by these analyses generated testable predictions
479 about the diets of many species for which we only have morphological data of their tenta-
480 cles. For example, the unique tentilla morphology of *Frillagalma* is predicted to render a
481 generalist diet, or one of the undescribed deep-sea physonect species examined is predicted

482 to be a fish specialist, which is congruent with its close phylogenetic relationship to other
483 piscivorous physonects. While the limited dataset used here is informative for generating
484 tentative hypotheses, the empirical dietary data are still scarce and insufficient to cast robust
485 predictions. This reveals the need to extensively characterize siphonophore diets and feeding
486 habits. In future work, we will test these ecological hypotheses and validate these models
487 by directly characterizing the diets of some of those siphonophore species. Predicting diet
488 using morphology is a powerful tool to reconstruct food web topologies from community
489 composition alone. In many of the ecological models found in the literature, interactions
490 among the oceanic zooplankton have been treated as a black box (Mitra 2009). The ability
491 to predict such interactions, including those of siphonophores and their prey, will enhance
492 the taxonomic resolution of nutrient-flow models constructed from plankton community
493 composition data.

494 Acknowledgements

495 This work was supported by the Society of Systematic Biologists (Graduate Student Award
496 to A.D.S.); the Yale Institute of Biospheric Studies (Doctoral Pilot Grant to A.D.S.); and
497 the National Science Foundation (Waterman Award to C.W.D., OCE-1829835 to C.W.D.,
498 OCE-1829805 to S.H.D.H., and OCE-1829812 to C. Anela Choy). A.D.S. was supported by
499 a Fulbright Spain Graduate Studies Scholarship.

500 **References**

- 501 Adams DC, Collyer M, Kaliontzopoulou A, Sherratt E. 2016. Geomorph: Software for
502 geometric morphometric analyses..
- 503 Bardi J, Marques AC. 2007. Taxonomic redescription of the portuguese man-of-war,
504 physalia physalis (cnidaria, hydrozoa, siphonophorae, cystonectae) from brazil. Iheringia
505 Série Zoologia 97:425–33.
- 506 Blomberg SP, Garland T, Ives AR. 2003. Testing for phylogenetic signal in comparative
507 data: Behavioral traits are more labile. Evolution 57:717–45.
- 508 Blyth CR. 1972. On simpson's paradox and the sure-thing principle. Journal of the
509 American Statistical Association 67:364–66.
- 510 Carré D. 1972. Study on development of cnidocysts in gastrozooids of muggiaeae kochi
511 (will, 1844) (siphonophora, calycophora). Comptes Rendus Hebdomadaires des Séances de
512 l'Academie des Sciences Serie D 275:1263.
- 513 Carré D, Carré C. 1980. On triggering and control of cnidocyst discharge. Marine &
514 Freshwater Behaviour & Phy 7:109–17.
- 515 Damian-Serrano A, Haddock SH, Dunn CW. 2020. The evolution of siphonophore tentilla
516 for specialized prey capture in the open ocean. PNAS 653345.
- 517 Dunn CW, Pugh PR, Haddock SH. 2005. Marrus claudanielis, a new species of deep-sea
518 physonect siphonophore (siphonophora, physonectae). Bulletin of Marine Science 76:699–714.
- 519 Felsenstein J. 1985. Phylogenies and the comparative method. The American Naturalist
520 125:1–15.
- 521 Haddock SH, Dunn CW, Pugh PR. 2005. A re-examination of siphonophore terminology
522 and morphology, applied to the description of two new prayine species with remarkable
523 bio-optical properties. Journal of the Marine Biological Association of the United Kingdom
524 85:695–707.
- 525 Harmon LJ, Weir JT, Brock CD, Glor RE, Challenger W. 2007. GEIGER: Investigating
526 evolutionary radiations. Bioinformatics 24:129–31.

- 527 Hessinger DA. 1988. Nematocyst venoms and toxins. In: The biology of nematocysts
528 Elsevier. pp. 333–68.
- 529 Hissmann K. 2005. In situ observations on benthic siphonophores (physonectae: Rhodali-
530 idae) and descriptions of three new species from indonesia and south africa. Systematics and
531 Biodiversity 2:223–49.
- 532 Ingram T, Mahler DL. 2013. SURFACE: Detecting convergent evolution from comparative
533 data by fitting ornstein-uhlenbeck models with stepwise akaike information criterion. Methods
534 in ecology and evolution 4:416–25.
- 535 Jombart T, Devillard S, Balloux F. 2010. Discriminant analysis of principal components:
536 A new method for the analysis of genetically structured populations. BMC genetics 11:94.
- 537 Mackie GO, Pugh PR, Purcell JE. 1987. Siphonophore Biology. Advances in Marine
538 Biology 24:97–262.
- 539 Mapstone GM. 2014. Global diversity and review of siphonophorae (cnidaria: Hydrozoa).
540 PLoS One 9:e87737.
- 541 Mariscal RN. 1974. Nematocysts..
- 542 Mitra A. 2009. Are closure terms appropriate or necessary descriptors of zooplankton
543 loss in nutrient–phytoplankton–zooplankton type models? Ecological Modelling 220:611–20.
- 544 Munro C, Siebert S, Zapata F, Howison M, Serrano AD, Church SH, Goetz FE, Pugh
545 PR, Haddock SH, Dunn CW. 2018. Improved phylogenetic resolution within siphonophora
546 (cnidaria) with implications for trait evolution. Molecular Phylogenetics and Evolution.
- 547 Pennell MW, FitzJohn RG, Cornwell WK, Harmon LJ. 2015. Model adequacy and the
548 macroevolution of angiosperm functional traits. The American Naturalist 186:E33–E50.
- 549 Pugh P. 1983. Benthic siphonophores: A review of the family rhodaliidai (siphonophora,
550 physonectae) Royal Society.
- 551 Pugh P. 2001. A review of the genus erenna bedot, 1904 (siphonophora, physonectae).
552 BULLETIN-NATURAL HISTORY MUSEUM ZOOLOGY SERIES 67:169–82.
- 553 Pugh P, Baxter E. 2014. A review of the physonect siphonophore genera halistemma

- 554 (family agalmatidae) and stephanomia (family stephanomiidae). Zootaxa 3897:1–111.
- 555 Pugh P, Haddock S. 2010. Three new species of remosiid siphonophore (siphonophora:
556 Physonectae). Journal of the Marine Biological Association of the United Kingdom 90:1119–
557 43.
- 558 Pugh P, Harbison G. 1986. New observations on a rare physonect siphonophore, lychna-
559 galma utricularia (claus, 1879). Journal of the Marine Biological Association of the United
560 Kingdom 66:695–710.
- 561 Pugh P, Youngbluth M. 1988. Two new species of prayine siphonophore (calycophorae,
562 prayidae) collected by the submersibles johnson-sea-link i and ii. Journal of Plankton Research
563 10:637–57.
- 564 Purcell J. 1981. Dietary composition and diel feeding patterns of epipelagic siphonophores.
565 Marine Biology 65:83–90.
- 566 Purcell JE. 1984. The functions of nematocysts in prey capture by epipelagic siphonophores
567 (coelenterata, hydrozoa). The Biological Bulletin 166:310–27.
- 568 Revell LJ. 2012. Phytools: An r package for phylogenetic comparative biology (and other
569 things). Methods in Ecology and Evolution 3:217–23.
- 570 Revell LJ, Chamberlain SA. 2014. Rphylip: An r interface for phylip. Methods in Ecology
571 and Evolution 5:976–81.
- 572 Siebert S, Pugh PR, Haddock SH, Dunn CW. 2013. Re-evaluation of characters in
573 apolemiidae (siphonophora), with description of two new species from monterey bay, california.
574 Zootaxa 3702:201–32.
- 575 Skaer R. 1988. The formation of cnidocyte patterns in siphonophores Academic Press
576 New York.
- 577 Skaer R. 1991. Remodelling during the development of nematocysts in a siphonophore.
578 In: Hydrobiologia Springer. pp. 685–89.
- 579 Sugiura N. 1978. Further analysts of the data by akaike's information criterion and the
580 finite corrections: Further analysts of the data by akaike's. Communications in Statistics-

- 581 Theory and Methods 7:13–26.
- 582 Thomason J. 1988. The allometry of nematocysts. In: The biology of nematocysts
583 Elsevier. pp. 575–88.
- 584 Totton AK, Bargmann HE. 1965. A synopsis of the siphonophora British Museum
585 (Natural History).
- 586 Uyeda JC, Zenil-Ferguson R, Pennell MW. 2018. Rethinking phylogenetic comparative
587 methods. Systematic Biology 67:1091–1109.
- 588 Wagner GP. 1996. Homologues, natural kinds and the evolution of modularity. American
589 Zoologist 36:36–43.
- 590 Werner B. 1965. Die nesselkapseln der cnidaria, mit besonderer berücksichtigung der
591 hydroida. Helgoländer wissenschaftliche Meeresuntersuchungen 12:1.
- 592 Winemiller KO, Fitzgerald DB, Bower LM, Pianka ER. 2015. Functional traits, convergent
593 evolution, and periodic tables of niches. Ecology letters 18:737–51.